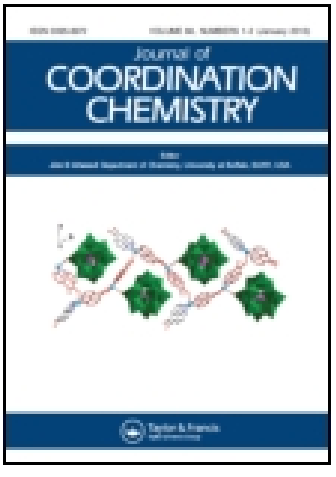

Journal of Coordination Chemistry
Publication details, including instructions for authors and subscription information:
http://www.tandfonline.com/loi/gcoo20

Disubstituted diphenyldithiophosphates of cadmium: synthesis, characterization, and single-crystal X-ray structure

Ruchi Khajuria[a], Sandeep Kumar[a], Atiya Syed[a], Gurvinder Kour[b], Sumati Anthal[b], Vivek K. Gupta[b], Rajni Kant[b] & Sushil Kumar Pandey[a]

[a] Department of Chemistry, University of Jammu, Jammu, India
[b] X-ray Crystallography Laboratory, Post-Graduate Department of Physics & Electronics, University of Jammu, Jammu, India

Accepted author version posted online: 26 Aug 2014.Published online: 16 Sep 2014.

To cite this article: Ruchi Khajuria, Sandeep Kumar, Atiya Syed, Gurvinder Kour, Sumati Anthal, Vivek K. Gupta, Rajni Kant & Sushil Kumar Pandey (2014) Disubstituted diphenyldithiophosphates of cadmium: synthesis, characterization, and single-crystal X-ray structure, Journal of Coordination Chemistry, 67:17, 2925-2941, DOI: 10.1080/00958972.2014.958473

To link to this article: http://dx.doi.org/10.1080/00958972.2014.958473

Journal of Coordination Chemistry, 2014
Vol. 67, No. 17, 2925–2941, http://dx.doi.org/10.1080/00958972.2014.958473

Disubstituted diphenyldithiophosphates of cadmium: synthesis, characterization, and single-crystal X-ray structure

RUCHI KHAJURIA†, SANDEEP KUMAR†, ATIYA SYED†, GURVINDER KOUR‡, SUMATI ANTHAL‡, VIVEK K. GUPTA‡, RAJNI KANT‡ and SUSHIL KUMAR PANDEY*†

†Department of Chemistry, University of Jammu, Jammu, India
‡X-ray Crystallography Laboratory, Post-Graduate Department of Physics & Electronics, University of Jammu, Jammu, India

(*Received 6 December 2013; accepted 14 July 2014*)

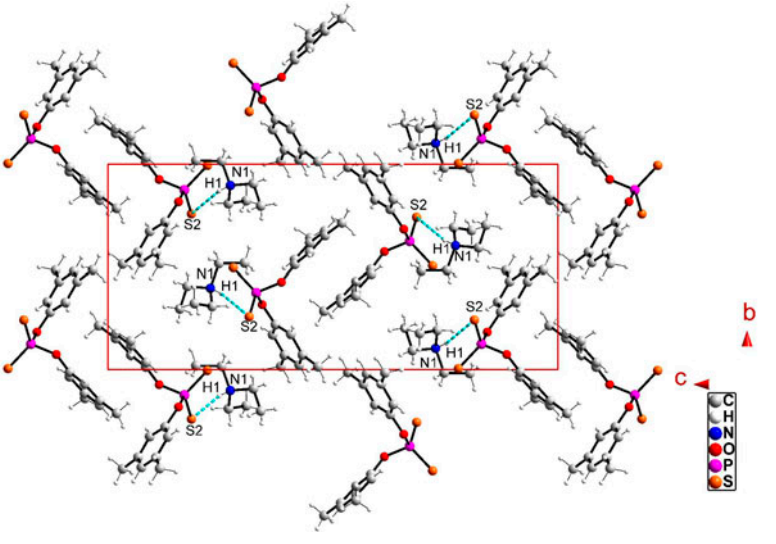

A series of new disubstituted diphenyldithiophosphate complexes of cadmium $[\{(ArO)_2PS_2\}_2Cd]$ (**9**–**12**) have been isolated in aqueous media while their donor stabilized adducts $[\{(ArO)_2PS_2\}_2Cd{\cdot}2C_5H_5N]$ (**13**–**16**) [(Ar = 2,4-$(CH_3)_2C_6H_3$, 2,5-$(CH_3)_2C_6H_3$, 3,4-$(CH_3)_2C_6H_3$ and 3,5-$(CH_3)_2C_6H_3$)] have been isolated in chloroform. These newly synthesized complexes were characterized by elemental analyses, IR and NMR (^1H, ^{13}C and ^{31}P) spectroscopic analyses. The dithiophosphate ligands are coordinated bidentate to the cadmium ion via the two thiolate sulfurs. The compounds $[\{(3,5\text{-}CH_3)_2C_6H_3O\}_2PS_2HNEt_3]$ (**4**) and $[\{(3,5\text{-}CH_3)_2C_6H_3O\}_2PS_2]_2Cd(NC_5H_5)_2$ (**16**) crystallize in the monoclinic system with space group $P2_1/c$. Single-crystal X-ray analysis of **4** reveals that phosphorus of the anion is tetrahedrally bonded to two S and two O atoms. The structure is stabilized by cation–anion N–H···S intermolecular hydrogen bond interactions. In **16**, two diphenyldithiophosphate ions are bidentate with both sulfurs coordinated to cadmium. Each forms a

*Corresponding author. Email: kpsushil@rediffmail.com

four-membered chelate ring in the equatorial plane. Two pyridines are axially coordinated to cadmium leading to octahedral geometry. The thermal properties of this complex have also been examined by combined DTA/DTG thermal analyses.

Keywords: Cadmium(II); Diphenyldithiophosphate; Crystal structure; Pyridine

1. Introduction

The chemistry of cadmium dithiolates continues to be a prominent area of research for emerging applications as precursors in metal organic chemical vapor deposition [1–3]. Recent work has established that cadmium dithiocarbamates may be useful precursors to form CdS nanowires and may have applications as nonlinear optical materials [4, 5]. Cadmium and its compounds have numerous applications; however, in recent years, the use of cadmium has declined, mainly due to concerns over the toxicity of cadmium and the introduction of regulations. Cadmium and its compounds are a substantial industrial and environmental pollutant [6] which seriously impairs erythropoiesis. Cadmium accumulates in humans throughout their lives [7], with a negative effect on human beings and also to soil micro-organisms [8–11]. The development of the efficient antidotes for cadmium intoxication has proven to be a task of considerable difficulty. Two types of chelating agents can affect antidotes for cadmium intoxication: uncharged vicinal dithiols [12] and dithiocarbamates [13, 14]. The affinity of 1,1-dithiolate ligands for cadmium was indicated by the fact that the ligands can be employed as scavengers for this toxic element in biological media.

Divalent d^{10} metal ions have various coordination geometries. While cadmium chemistry of dithioacid based ligands like dithiocarbamate has been the subject of continuous study, the corresponding cadmium dithiophosphate chemistry has not been developed. The versatile bonding, structural features, and fascinating chemical as well as electrochemical reactivities of cadmium dialkyldithiophosphate complexes prompted us to make a systematic study of cadmium diphenyldithiophosphates. During the past four decades, molecular structures of cadmium(II) complexes are known for *O,O′*-dialkyldithiophosphate ligands [15–21]. In these complexes, *O,O′*-dialkyldithiophosphate ligands adopt a bridging coordination to form binuclear structures $[Cd_2\{S_2P(OR)_2\}_4]$ (R = *s*-Bu [16], Cy [17], *i*-Pr [18, 19]) and polynuclear structures $[Cd\{S_2P(OR)_2\}_2]_n$ (R = *i*-Bu) [20], (*n*-Pr and *n*-Bu) [21], eight-membered metallocycles $[Cd_2S_4P_2]$ are formed in both bi- and polynuclear complexes.

These eight-membered metallocycles are easily destroyed by nitrogen donors in solution and result in adducts with distorted octahedral geometry around cadmium, such as $[Cd\{S_2P(OR)_2\}_2 \cdot L_n]$ (R = *i*-Pr, L = phen, n = 1 [22]; R = Et, L = hexamethylenetetramine, n = 2 [23]; R = *i*-Pr, L = py, n = 2 [24]). Herein, we report the synthesis, spectroscopic and structural properties of disubstituted diphenyldithiophosphate ligands with cadmium(II) and donor stabilized complexes.

2. Experimental

2.1. *Materials and instrumentation*

Solvents were distilled and dried over sodium before use. Chloroform (Thomas Baker) was dried over P_2O_5. All dimethylphenols (Sigma Aldrich) were used as supplied.

$Cd(NO_3)_2{\cdot}4H_2O$ (Sigma Aldrich) was used as received. Triethylammonium salts of *O,O′*-disubstituted diphenyldithiophosphates were synthesized according to a literature procedure used for the synthesis of ditolyl dithiophosphates [25]. Moisture was carefully excluded during the experimental manipulations for the synthesis of ligands by using standard Schlenk techniques. Cadmium and chloride were estimated gravimetrically as $[Cd(C_5H_5N)_2](SCN)_2]$ and estimated volumetrically by Volhard's method, respectively [26]. Elemental analyses (C, H, N, S) were conducted using the Elemental Analyser Vario EL-III (Indian Institute of Integrative Medicine, Jammu). Infrared spectra were recorded from 4000 to 200 cm^{-1} on a Perkin–Elmer spectrum RX1 FT-IR spectrophotometer (Sophisticated Analytical Instrumentation Facility, Panjab University, Chandigarh). ^1H, ^{13}C and ^{31}P (proton-decoupled) NMR spectra were recorded in $CDCl_3$ and DMSO-d_6 using TMS as internal reference and H_3PO_4 (85%) as external reference on a Bruker Avance III 400 MHz. All chemical shifts are reported in δ units downfield from TMS. TGA/DTA was recorded on a Linseis STA PT-1000 thermal analyser at a heating rate of 10 °C/min in air. NMR spectral and thermal analyses were carried out at the Department of Chemistry, University of Jammu, Jammu.

2.2. *Synthesis of ligands*

2.2.1. $[\{(2,4\text{-}CH_3)_2C_6H_3O\}_2PS_2HNEt_3]$ (1). A toluene solution (~40 mL) of 2,4-dimethylphenol (4.39 g, 35.93 mM) was added dropwise to a toluene (~30 mL) suspension of P_2S_5 (2.00 g, 8.99 mM) with constant stirring. After stirring the contents for 5–7 min at ~40 °C, a toluene solution (~40 mL) of Et_3N (1.82 g, 17.98 mM) was added dropwise to it with constant stirring. All the P_2S_5 was dissolved in 15–20 min, resulting in a clear colorless solution and evolution of H_2S was observed. Evaporation of excess toluene under reduced pressure resulted in formation of **1** as a white crystalline solid in quantitative yield. The resulting solid was dissolved in toluene and a few drops of *n*-hexane were added for recrystallization at room temperature. Yield: 96% (7.52 g); m.p. 60−62 °C (dec); Anal. Calcd for $C_{16}H_{18}O_2PS_2HNEt_3$ (M.W. 439.61): C, 60.11; H, 7.80; S, 14.59; N, 3.19%. Found: C, 60.07; H, 7.77; S, 14.54; N, 3.13%. IR (KBr): 3397 b [N–H], 1196 s [ν(P)–O–C], 870 s [νP–O–(C)], 673 s [νP=S], 580 m [νP–S] cm^{-1}.

2.2.2. $[\{(2,5\text{-}CH_3)_2C_6H_3O\}_2PS_2HNEt_3]$ (2). Compound **2** was prepared as white crystalline solid by similar procedure as described above for **1** using 2,5-dimethylphenol (4.39 g, 35.93 mM), P_2S_5 (2.00 g, 8.99 mM), and Et_3N (1.82 g, 17.98 mM). The resulting solid was dissolved in toluene and a few drops of *n*-hexane were added for recrystallization at room temperature. Yield: 97% (7.60 g); m.p. 62–64 °C (dec); Anal. Calcd for $C_{16}H_{18}O_2PS_2HNEt_3$ (M.W. 439.61): C, 60.11; H, 7.80; S, 14.59; N, 3.19%. Found: C, 60.08; H, 7.75; S, 14.55; N, 3.14%. IR (KBr): 3413 b [N–H], 1150 s [ν(P)–O–C], 877 s [νP–O–(C)], 688 s [νP=S], 575 m [νP–S] cm^{-1}.

2.2.3. $[\{(3,4\text{-}CH_3)_2C_6H_3O\}_2PS_2HNEt_3]$ (3). Compound **3** was prepared as white crystalline solid by similar procedure as described for **1** using 3,4-dimethylphenol (4.39 g, 35.93 mM), P_2S_5 (2.00 g, 8.99 mM) and Et_3N (1.82 g, 17.98 mM). The resulting solid was dissolved in toluene and a few drops of *n*-hexane were added for recrystallization at room

temperature. Yield: 98% (7.68 g); m.p. 61–63 °C (dec); Anal. Calcd for $C_{16}H_{18}O_2PS_2H$-NEt_3 (M.W. 439.61): C, 60.11; H, 7.80; S, 14.59; N, 3.19%. Found: C, 60.07; H, 7.76; S, 14.54; N, 3.16%. IR (KBr): 3399 b [N–H], 1148 s [ν(P)–O–C], 856 s [νP–O–(C)], 672 s [νP=S], 574 m [νP–S] cm^{-1}.

2.2.4. [{(3,5-CH_3)$_2$$C_6H_3O$}$_2$$PS_2HNEt_3$] (4). Compound **4** was prepared as white crystalline solid by similar procedure as described for **1** using 3,5-dimethylphenol (4.39 g, 35.93 mM), P_2S_5 (2.00 g, 8.99 mM), and Et_3N (1.82 g, 17.98 mM). The resulting solid was dissolved in toluene and a few drops of *n*-hexane were added for recrystallization at room temperature. Yield: 97% (7.60 g); m.p. 65–67 °C (dec); Anal. Calcd for $C_{16}H_{18}O_2PS_2H$-NEt_3 (M.W. 439.61): C, 60.11; H, 7.80; S, 14.59; N, 3.19%. Found: C, 60.09; H, 7.75; S, 14.53; N, 3.15%. IR (KBr): 3431 b [N–H], 1141 s [ν(P)–O–C], 843 s [νP–O–(C)], 688 s [νP=S], 578 m [νP–S] cm^{-1}.

2.2.5. [{(2,4-CH_3)$_2$$C_6H_3O$}$_2$$PS_2Na$] (5). A weighed amount of sodium metal (0.42 g, 17.87 mM) was added to a toluene solution of triethylammonium salt [{2,4-$(CH_3)_2C_6H_3O\}_2PS_2HNEt_3$] (**1**) and the mixture was stirred for 3 h at ~55 °C, which resulted in formation of white precipitates. The contents were cooled and then filtered by a funnel fitted with a G-4 sintered disk. Finally, the residue was dried under reduced pressure giving **5** as a white solid. Yield: 95.5% (6.18 g); m.p. 190–192 °C (dec); Anal. Calcd for $C_{16}H_{18}O_2PS_2Na$: C, 53.32; H, 5.03; S, 17.79%. Found: C, 53.29; H, 4.95; S, 17.77%. IR (KBr): 1172 s [ν(P)–O–C], 832 s [νP–O–(C)], 652 s [νP═S], 570 m [νP–S] cm^{-1}.

2.2.6. [{(2,5-CH_3)$_2$$C_6H_3O$}$_2$$PS_2Na$] (6). Compound **6** was prepared as white powdery solid by similar procedure as described above for **5** using triethylammonium salt [{2,5-$(CH_3)_2C_6H_3O\}_2PS_2HNEt_3$] (**2**) and sodium metal (0.42 g, 17.87 mM). Yield: 96.3% (6.24 g); m.p. 192–194 °C (dec); Anal. Calcd for $C_{16}H_{18}O_2PS_2Na$: C, 53.32; H, 5.03; S, 17.79%. Found: C, 53.30; H, 4.99; S, 17.74%. IR (KBr): 1159 s [ν(P)–O–C], 846 s [νP–O–(C)], 670 s [νP═S], 556 m [νP–S] cm^{-1}.

2.2.7. [{(3,4-CH_3)$_2$$C_6H_3O$}$_2$$PS_2Na$] (7). Compound **7** was prepared as white powdery solid by similar procedure as described for **5** using triethylammonium salt [{3,4-$(CH_3)_2C_6H_3O\}_2PS_2HNEt_3$] (**3**) and sodium metal (0.42 g, 17.87 mM). Yield: 97.6% (6.34 g); m.p. 190–192 °C (dec); Anal. Calcd for $C_{16}H_{18}O_2PS_2Na$: C, 53.32; H, 5.03; S, 17.79%. Found: C, 53.29; H, 4.96; S, 17.71%. IR (KBr): 1152 s [ν(P)–O–C], 842 s [νP–O–(C)], 659 s [νP=S], 563 m [νP–S] cm^{-1}.

2.2.8. [{(3,5-CH_3)$_2$$C_6H_3O$}$_2$$PS_2Na$] (8). Compound **8** was prepared as white powdery solid by similar procedure as described for **5** using triethylammonium salt [{3,5-$(CH_3)_2C_6H_3O\}_2PS_2HNEt_3$] (**4**) and sodium metal (0.42 g, 17.87 mM). Yield: 97.4% (6.31 g); m.p. 194–196 °C (dec); Anal. Calcd for $C_{16}H_{18}O_2PS_2Na$: C, 53.32; H, 5.03; S, 17.79%. Found: C, 53.27; H, 4.97; S, 17.76%. IR (KBr): 1149 s [ν(P)–O–C], 836 s [νP–O–(C)], 661 s [νP═S], 559 m [νP–S] cm^{-1}.

2.3. *Synthesis of complexes*

2.3.1. [{(2,4-CH_3)$_2$$C_6H_3O$}$_2$$PS_2$]$_2$Cd (9). To an aqueous solution of $Cd(NO_3)_2 \cdot 4H_2O$ (0.42 g, 1.36 mM), an aqueous solution of [{(2,4-CH_3)$_2$$C_6H_3O$}$_2$$PS_2Na$] (1.00 g, 2.77 mM) was added in 1 : 2 M ratio with constant stirring at room temperature. A white solid mass precipitated out immediately. After 30 min of stirring, the reaction contents were filtered using an SG-4 sintered glass crucible to obtain [{(2,4-CH_3)$_2$$C_6H_3O$}$_2$$PS_2$]$_2$Cd (**9**) as white solid. The resulting solid was recrystallized from a chloroform/*n*-hexane mixture at room temperature. Yield: 91.2% (0.97 g); m.p. 142–144 °C (dec); Anal. Calcd for $C_{32}H_{36}O_4P_2S_4Cd$ (M.W. 787.24): C, 48.82; H, 4.61; S, 16.29; Cd, 14.28. Found: C, 48.79; H, 4.59; S, 16.27; Cd, 14.25. IR (KBr): 1088 s [ν(P)–O–C], 939 s [νP–O–(C)], 653 s [νP–S]$_{asym}$, 583 m [νP–S]$_{sym}$, 262 w [νCd–S] cm^{-1}.

2.3.2. [{(2,5-CH_3)$_2$$C_6H_3O$}$_2$$PS_2$]$_2$Cd (10). Complex **10** was obtained as white solid by similar procedure as described for **9** using $Cd(NO_3)_2 \cdot 4H_2O$ (0.42 g, 1.36 mM) and [{(2,5-CH_3)$_2$$C_6H_3O$}$_2$$PS_2Na$] (1.00 g, 2.77 mM). The resulting solid was recrystallized from a chloroform/*n*-hexane mixture at room temperature. Yield: 93.4% (0.99 g); m.p. 144–146 °C (dec); Anal. Calcd for $C_{32}H_{36}O_4P_2S_4Cd$ (M.W. 787.24): C, 48.82; H, 4.61; S, 16.29; Cd, 14.28. Found: C, 48.76; H, 4.56; S, 16.25; Cd, 14.24. IR (KBr): 1097 s [ν(P)–O–C], 952 s [νP–O–(C)], 669 s [νP–S]$_{asym}$, 608 m [νP–S]$_{sym}$, 263 w [νCd–S] cm^{-1}.

2.3.3. [{(3,4-CH_3)$_2$$C_6H_3O$}$_2$$PS_2$]$_2$Cd (11). Complex **11** was obtained as white solid by similar procedure as described for **9** using $Cd(NO_3)_2 \cdot 4H_2O$ (0.42 g, 1.36 mM) and [{(3,4-CH_3)$_2$$C_6H_3O$}$_2$$PS_2Na$] (1.00 g, 2.77 mM). The resulting solid was recrystallized from a chloroform/*n*-hexane mixture at room temperature. Yield: 91.8% (0.98 g); m.p. 143–145 °C (dec); Anal. Calcd for $C_{32}H_{36}O_4P_2S_4Cd$ (M.W. 787.24): C, 48.82; H, 4.61; S, 16.29; Cd, 14.28. Found: C, 48.80; H, 4.59; S, 16.26; Cd, 14.22. IR (KBr): 1124 s [ν(P)–O–C], 970 s [νP–O–(C)], 668 s [νP–S]$_{asym}$, 639 m [νP–S]$_{sym}$, 264 w [νCd–S] cm^{-1}.

2.3.4. [{(3,5-CH_3)$_2$$C_6H_3O$}$_2$$PS_2$]$_2$Cd (12). Complex **12** was obtained as white solid by similar procedure as described for **9** using $Cd(NO_3)_2 \cdot 4H_2O$ (0.42 g, 1.36 mM) and [{(3,5-CH_3)$_2$$C_6H_3O$}$_2$$PS_2Na$] (1.00 g, 2.77 mM). The resulting solid was recrystallized from a chloroform/*n*-hexane mixture at room temperature. Yield: 92.6% (0.99 g); m.p. 144–146 °C (dec); Anal. Calcd for $C_{32}H_{36}O_4P_2S_4Cd$ (M.W. 787.24): C, 48.82; H, 4.61; S, 16.29; Cd, 14.28. Found: C, 48.77; H, 4.58; S, 16.27; Cd, 14.25. IR (KBr): 1101 s [ν(P)–O–C], 947 s [νP–O–(C)], 653 s [νP–S]$_{asym}$, 593 m [νP–S]$_{sym}$, 260 w [νCd–S] cm^{-1}.

2.4. *Synthesis of adducts*

2.4.1. [{(2,4-CH_3)$_2$$C_6H_3O$}$_2$$PS_2$]$_2$Cd($NC_5H_5$)$_2$ (13). To a chloroform solution of [{(2,4-CH_3)$_2$$C_6H_3O$}$_2$$PS_2$]$_2$Cd (**9**) (1.00 g, 1.27 mM), chloroform solution of pyridine (0.20 g, 2.53 mM) was added dropwise with constant stirring at room temperature. Colorless solution changes to pale yellow within 15 min. The contents were stirred for a further 30 min at room temperature. The solvent was then evaporated under vacuum, which results in **13** as pale yellow solid. The resulting solid was recrystallized from a chloroform/*n*-hexane

mixture at room temperature. Yield: 88.6% (1.06 g); m.p. 162–164 °C (dec); Anal. Calcd for $C_{42}H_{46}N_2O_4P_2S_4Cd$: C, 53.36; H, 4.90; S, 13.57; N, 2.96; Cd, 11.89. Found: C, 53.34; H, 4.87; S, 13.55; N, 2.93; Cd, 11.86. IR (KBr): 1116 s [ν(P)–O–C], 996 s [νP–O–(C)], 642 s [νP–S]$_{asym}$, 586 m [νP–S]$_{sym}$, 260 w [νCd–S], 540 w [νCd–N] cm^{-1}.

2.4.2. $[\{(2,5\text{-}CH_3)_2C_6H_3O\}_2PS_2]_2Cd(NC_5H_5)_2$ (14). Complex **14** was obtained as pale yellow solid by similar procedure as described for **13** using pyridine (0.20 g, 2.53 mM) and $[\{(2,5\text{-}CH_3)_2C_6H_3O\}_2PS_2]_2Cd$ (**10**) (1.00 g, 1.27 mM). The resulting solid was recrystallized from a chloroform/*n*-hexane mixture at room temperature. Yield: 87.4% (1.04 g); m.p. 164–166 °C (dec); Anal. Calcd for $C_{42}H_{46}N_2O_4P_2S_4Cd$: C, 53.36; H, 4.90; S, 13.57; N, 2.96; Cd, 11.89. Found: C, 53.32; H, 4.86; S, 13.56; N, 2.94; Cd, 11.86. IR (KBr): 1141 s [ν(P)–O–C], 960 s [νP–O–(C)], 645 s [νP–S]$_{asym}$, 594 m [νP–S]$_{sym}$, 263 w [νCd–S], 531 w [νCd–N] cm^{-1}.

2.4.3. $[\{(3,4\text{-}CH_3)_2C_6H_3O\}_2PS_2]_2Cd(NC_5H_5)_2$ (15). Complex **15** was obtained as pale yellow solid by similar procedure as described for **13** using pyridine (0.20 g, 2.53 mM) and **11** (1.00 g, 1.27 mM). The resulting solid was recrystallized from a chloroform/*n*-hexane mixture at room temperature. Yield: 88.3% (1.05 g); m.p. 162–164 °C (dec); Anal. Calcd for $C_{42}H_{46}N_2O_4P_2S_4Cd$: C, 53.36; H, 4.90; S, 13.57; N, 2.96; Cd, 11.89. Found: C, 53.34; H, 4.83; S, 13.53; N, 2.93; Cd, 11.83. IR (KBr): 1127 s [ν(P)–O–C], 957 s [νP–O–(C)], 672 s [νP–S]$_{asym}$, 621 m [νP–S]$_{sym}$, 261 w [νCd–S], 533 w [νCd–N] cm^{-1}.

2.4.4. $[\{(3,5\text{-}CH_3)_2C_6H_3O\}_2PS_2]_2Cd(NC_5H_5)_2$ (16). Complex **16** was obtained as pale yellow solid by similar procedure as described for **13** using pyridine (0.20 g, 2.53 mM) and **12** (1.00 g, 1.27 mM). The resulting solid was recrystallized from a chloroform/*n*-hexane mixture at room temperature. Yield: 89.4% (1.07 g); m.p. 163–165 °C (dec); Anal. Calcd for $C_{42}H_{46}N_2O_4P_2S_4Cd$: C, 53.36; H, 4.90; S, 13.57; N, 2.96; Cd, 11.89. Found: C, 53.33; H, 4.86; S, 13.52; N, 2.92; Cd, 11.84. IR (KBr): 1128 s [ν(P)–O–C], 954 s [νP–O–(C)], 633 s [νP–S]$_{asym}$, 615 m [νP–S]$_{sym}$, 265 w [νCd–S], 521 w [νCd–N] cm^{-1}.

2.5. *X-ray crystallography*

Crystallization of **4** was executed by dissolving solid in toluene and a few drops of *n*-hexane were added, then solvents were allowed to evaporate slowly to obtain white single crystals. The crystallization of **16** was achieved by slow evaporation of chloroform/*n*-hexane mixture which resulted in pale yellow crystals at room temperature. The structures of **4** and **16** were determined by single-crystal X-ray diffraction analysis. X-ray intensity data were collected by using an X'calibur Oxford Diffraction single-crystal X-ray diffractometer with graphite monochromated Mo K_α radiation (λ = 0.71073 Å) and reduced with CrysAlis *RED* [27]. Data were corrected for Lorentz, polarization and absorption factors. The structure was solved by direct methods using SHELXS97 and refined by SHELXL97 [28]. The geometry of the molecule is determined by PLATON [29] and PARST [30] software. All hydrogens were geometrically fixed and allowed to ride on their parent carbon, with C–H distances of 0.93–0.97 Å and with $U_{iso}(H) = 1.2U_{eq}(C)$, except for the methyl group where $U_{iso}(H) = 1.5U_{eq}(C)$. The crystallographic data are summarized in table 1.

Table 1. Crystal data and structure refinements for **4** and **16**.

Compound	**4**	**16**
Crystal system	Monoclinic	Monoclinic
Space group	$P2_1/c$	$P2_1/c$
Temperature, K	293(2)	293(2)
Empirical formula	$C_{22}H_{34}NO_2PS_2$	$C_{42}H_{46}CdN_2O_4P_2S_4$
Z	4	2
Formula weight	439.59	945.39
a (Å)	8.1973(7)	12.0398(2)
b (Å)	11.6205(8)	14.4082(3)
c (Å)	25.6019(22)	15.3752(2)
α (°)	90.00	90.00
β (°)	93.769(7)	125.4560(10)
γ (°)	90.00	90.00
V (Å^3)	2433.48(12)	2172.57(8)
D_{Calcd} (g/cm^3)	1.20	1.445
F (0 0 0)	943.9	972
θ Range for data collection (°)	3.60–26.00	3.55–27.00
No. of collected reflections	9823	36,504
No. of unique reflections	4781	4736
No. of data/restraints/parameters	4781/0/264	4736/0/273
R_1, wR_2 [$I > 2\sigma(I)$]	0.0624, 0.1382	0.0295, 0.0728
R_1, wR_2 (all data)	0.0944, 0.1600	0.0381, 0.0805
Goodness-of-fit on F^2	1.037	1.112
Largest diff. peak/hole (e Å^{-3})	0.412/−0.31	0.488/−0.520
CCDC No.	971866	971951

3. Results and discussion

Literature reports describe the isolation of phenyl/tolyl dithiophosphates [25]. However, there is no report available so far of similar compounds having disubstituted phenyl moiety. Triethylammonium salt of disubstituted diphenyldithiophosphates has been isolated for the first time by a facile reaction of 2,4-, 2,5-, 3,4- or 3,5-dimethylphenol with P_2S_5 in the presence of triethylamine in 4 : 1 : 2 M ratio in toluene at room temperature. The triethylammonium salts corresponding to $(ArO)_2PS_2HNEt_3$, where Ar = 2,4-$(CH_3)_2C_6H_3$ (**1**), 2,5-$(CH_3)_2C_6H_3$ (**2**), 3,4-$(CH_3)_2C_6H_3$ (**3**), and 3,5-$(CH_3)_2C_6H_3$ (**4**), are obtained as white crystalline solid in quantitative yield after removing of excess solvent (scheme 1).

These triethylammonium salts (**1**–**4**) are fairly soluble in common organic solvents like toluene, chloroform, methylene dichloride or benzene and are insoluble in carbon tetrachloride or *n*-hexane. The triethylammonium salts could easily be converted into sodium salts as white solids by direct reaction with sodium metal in toluene in equimolar ratio under strictly anhydrous atmosphere (scheme 2).

Sodium salts are soluble in water, DMSO, methanol, and ethanol, sparingly soluble in chloroform, and insoluble in most other hydrocarbon solvents.

$$4ArOH + P_2S_5 + 2Et_3N \xrightarrow[-H_2S]{\text{Toluene}} \underset{(\mathbf{1}\text{-}\mathbf{4})}{2(ArO)_2PS_2HNEt_3}$$

[Ar = 2,4-$(CH_3)_2C_6H_3$ (**1**), 2,5-$(CH_3)_2C_6H_3$ (**2**), 3,4-$(CH_3)_2C_6H_3$ (**3**) and 3,5-$(CH_3)_2C_6H_3$ (**4**)]

Scheme 1.

Scheme 2.

Cadmium diphenyldithiophosphates [{$(ArO)_2PS_2$}$_2$Cd] (Ar = 2,4-$(CH_3)_2C_6H_3$, 2,5-$(CH_3)_2C_6H_3$, 3,4-$(CH_3)_2C_6H_3$, and 3,5-$(CH_3)_2C_6H_3$) (**9**–**12**) have been isolated as white solid by the reaction of sodium salts of *O*,*O′*-diphenyldithiophosphoric acids (**5**–**8**) and cadmium nitrate tetrahydrate, $Cd(NO_3)_2{\cdot}4H_2O$, in 2 : 1 M stoichiometry in water (scheme 3).

The donor stabilized cadmium diphenyldithiophosphates [{$(ArO)_2PS_2$}$_2$Cd$(NC_5H_5)_2$] (Ar = 2,4-$(CH_3)_2C_6H_3$, 2,5-$(CH_3)_2C_6H_3$, 3,4-$(CH_3)_2C_6H_3$, and 3,5-$(CH_3)_2C_6H_3$) (**13**–**16**) were prepared by the reaction of cadmium diphenyldithiophosphates (**9**–**12**) with pyridine in 1 : 2 stoichiometry in chloroform (scheme 4).

All these complexes and adducts are soluble in common organic solvents and insoluble in solvents like *n*-hexane and carbon tetrachloride.

3.1. *IR spectra*

IR spectra of **1**–**16** were interpreted on the basis of relevant literature reports [25, 31–34]. IR spectra have a broad absorption for [νN–H] at 3431–3397 cm^{-1} in **1**–**4**, while these absorptions were absent in **5**–**8**. In **1**–**8**, [ν(P)–O–C] and [νP–O–(C)] were at 1196–1141 and 877–832 cm^{-1}, respectively. Sharp to medium intensity bands at 688–652 and 580–556 cm^{-1} are assignable to [νP=S] and [νP–S] (asymmetric and symmetric) vibrations. Comparison of IR spectra of the complexes and donor stabilized complexes with starting materials has also shown significant changes. Bands due to [νN–H] vibrations are absent in **9**–**16**. Two strong bands were observed at 1141–1088 and 996–939 cm^{-1} in **9**–**16**, which may be ascribed to [ν(P)–O–C] and [νP–O–(C)] of dimethyl diphenyldithiophosphate,

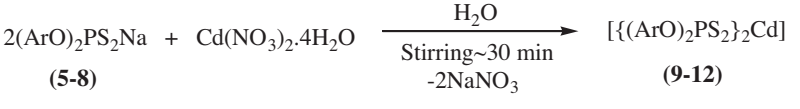

[Ar = 2,4-$(CH_3)_2C_6H_3$ (**9**), 2,5-$(CH_3)_2C_6H_3$ (**10**), 3,4-$(CH_3)_2C_6H_3$ (**11**) and 3,5-$(CH_3)_2C_6H_3$ (**12**)]

Scheme 3.

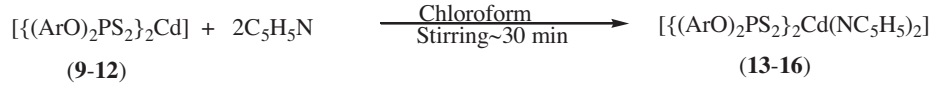

[Ar = 2,4-$(CH_3)_2C_6H_3$ (**13**), 2,5-$(CH_3)_2C_6H_3$ (**14**), 3,4-$(CH_3)_2C_6H_3$ (**15**) and 3,5-$(CH_3)_2C_6H_3$ (**16**)]

Scheme 4.

respectively. The regions of IR spectra for P–S are of particular interest. Bands for $[\nu P–S]_{asym}$ and $[\nu P–S]_{sym}$ of diphenyldithiophosphate in **9**–**16** were observed at 672–633 and 639–583 cm^{-1}, respectively. This shift and appearance of closely spaced bands arising from $\nu(PS_2)$ vibrations in **9**–**16** are quite diagnostic to propose bidentate bonding of dithio moiety with cadmium. Appearance of new bands of νCd–S (in comparison to free ligand) at 265–260 cm^{-1} indicates formation of cadmium–sulfur bonds [31]. The presence of bound pyridine to cadmium via nitrogen in **13**–**16** can be supported by the existence of a band at 540–521 cm^{-1}, assigned to νCd–N [32, 33].

3.2. *^{1}H, ^{13}C and ^{31}P NMR spectra*

^{1}H NMR spectra of **1**–**16** exhibited phenyl and pyridine proton signals with the expected peak multiplicities (table 2). For **9**–**16** chemical shifts of the methyl protons of the phenyl rings were observed at 2.14–2.36 ppm as a very sharp 12 proton singlet (**9**–**11** and **13**–**15**) and a 24 proton singlet in **12** and **16**. The aromatic protons of the phenyl groups were observed at 6.77–7.37 ppm with their characteristic splitting patterns. The chemical shifts for protons due to pyridine are observed at 7.21–8.55 ppm.

The ^{13}C NMR spectral data show the chemical shifts expected for the carbons present in the molecule (table 2). ^{13}C NMR spectra of **9**–**12** and adducts **13**–**16** show the chemical shifts of carbons of phenyl rings with a marginal shift in their values compared to the parent ligands (**5**–**8**). The chemical shift for the methyl ($–CH_3$) carbon, attached to phenyl, was found at 16.61–21.29 ppm. The carbon nuclei of the aryl groups have resonances at 118.69–139.08 ppm. The chemical shifts for C–O carbons were observed at 142.29–151.58 ppm. The carbons on the pyridine rings in **13**–**16** have three peaks at 122.46–149.69 ppm.

^{31}P NMR spectra (proton-decoupled) displayed a single resonance in each case. The ^{31}P NMR spectra of **9**–**12** have a singlet in each case in the upfield region 101.02–101.86 ppm compared to the parent compounds (106.02–107.48 ppm) with a difference of 5–6 ppm. This shift may be attributed to bidentate dithiophosphate [35]. Adducts **13**–**16** showed the ^{31}P chemical shift as a singlet in the downfield region 104.23–106.12 ppm compared to **9**–**12** with a difference of 3–5 ppm, which can be attributed to binding of two pyridines leading to six coordinate Cd. Occurrence of a singlet in each case indicated the equivalent nature of phosphorus nuclei in the molecule. More upfield shift was observed in four coordinate **9**–**12** than six coordinate **13**–**16** compared to the parent ligands. A summary of ^{1}H, ^{13}C and ^{31}P NMR data is presented in table 2.

3.3. *Molecular and crystal structures of [{(3,5-$(CH_3)_2C_6H_3O$}$_2PS_2HNEt_3$] (4) and [{(3,5-$(CH_3)_2C_6H_3O$}$_2PS_2$]$_2$Cd(NC_5H_5)$_2$ (16)*

ORTEP [36] view of triethylammonium salt **4** and adduct **16** with atomic labeling is shown in figures 1 and 2, respectively. Selected bond lengths and angles of both compounds are shown in tables 3 and 4, respectively. In the ORTEP diagram (figure 1), the expected distorted tetrahedral environment around phosphorus can be clearly seen with two sulfurs and two oxygens bound to phosphorus [figure 3(a)]. Compound **4** consists of triethyl ammonium and *O,O′*-bis[3,5-dimethylphenyl]dithiophosphate, connected through N1–H1···S2 intermolecular hydrogen bond (figure 4). The N1–H1 bond length is fixed at 0.94 Å, while the N1–S2 distance refines to 3.20(3) Å. This N1–S2 distance of 3.20(3) compares well

Table 2. ^{1}H, ^{13}C and ^{31}P NMR spectroscopic data of **1–16**.

S. No.	Compounds	^{1}H, ^{13}C and ^{31}P Chemical shift (δ)
1	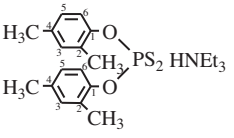	^{1}H NMR ($CDCl_3$, ppm): 1.25 (t, J = 14.4 Hz, 9H, CH_3 of Et_3N), 2.28 (s, 6H, 2-CH_3), 2.33 (s, 6H, 4-CH_3), 3.12 (q, 6H, CH_2 of Et_3N), 6.98 (d, J = 8 Hz, 2H, H_6), 7.00 (d, J = 8 Hz, 2H, H_5), 7.55 (s, 2H, H_3), 9.32 (s, 1H, –NH); ^{13}C NMR ($CDCl_3$, ppm): 8.55 (CH_3 of Et_3N), 17.48 (2-CH_3), 20.82 (4-CH_3), 46.18 (CH_2 of Et_3N), 114.96 (C_6), 121.47 (C_2–CH_3), 127.21 (C_5), 130.59 (C_4–CH_3), 133.18 (C_3), 151.97 (C1–O); ^{31}P NMR ($CDCl_3$, ppm): 106.95 (s)
2	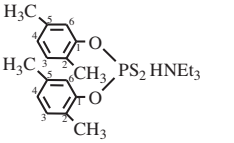	^{1}H NMR ($CDCl_3$, ppm): 1.25 (t, J = 14.4 Hz, 9H, CH_3 of Et_3N), 2.17 (s, 6H, 2-CH_3), 2.22 (s, 6H, 5-CH_3), 3.12 (q, 6H, CH_2 of Et_3N), 6.77 (d, J = 7.6 Hz, 2H, H_3), 7.02 (d, J = 7.6 Hz, 2H, H_4), 7.41 (s, 2H, H_6), 9.03 (s, 1H, –NH); ^{13}C NMR ($CDCl_3$, ppm): 8.53 (CH_3 of Et_3N), 16.63 (2-CH_3), 20.90 (5-CH_3), 46.28 (CH_2 of Et_3N), 121.46 (C_6), 126.64 (C_4), 127.32 (C_2–CH_3), 131.11 (C_3), 136.83 (C_5–CH_3), 149.56 (C_1–O); ^{31}P NMR ($CDCl_3$, ppm): 106.40 (s)
3	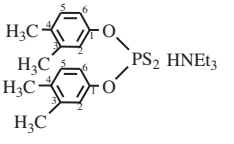	^{1}H NMR ($CDCl_3$, ppm): 1.26 (t, J = 14.4 Hz, 9H, CH_3 of Et_3N), 2.21 (s, 6H, 3-CH_3), 2.23 (s, 6H, 4-CH_3), 3.13 (q, 6H, CH_2 of Et_3N), 7.06 (d, J = 7.6 Hz, 2H, H_6), 7.17 (s, 2H, H_2), 7.37 (d, J = 8 Hz, 2H, H_5), 9.20 (s, 1H, –NH); ^{13}C NMR ($CDCl_3$, ppm): 8.57 (CH_3 of Et_3N), 19.12 (4-CH_3), 19.96 (3-CH_3), 46.31 (CH_2 of Et_3N), 116.77 (C_6), 119.18 (C_2), 130.30 (C_4–CH_3), 132.09 (C_5), 137.14 (C_3–CH_3), 150.56 (C_1–O); ^{31}P NMR ($CDCl_3$, ppm): 106.02 (s)
4	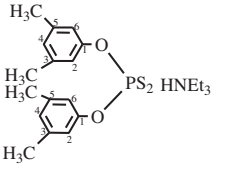	^{1}H NMR ($CDCl_3$, ppm): 1.29 (t, J = 14.4 Hz, 9H, CH_3 of Et_3N), 2.29 (s, 12H, 3,5-$(CH_3)_2$), 3.15 (q, 6H, CH_2 of Et_3N), 6.75 (s, 4H, $H_{2,6}$), 7.03 (s, 2H, H_4), 9.25 (s, 1H, –NH); ^{13}C NMR ($CDCl_3$, ppm): 8.50 (CH_3 of Et_3N), 21.35 (3,5-$(CH_3)_2$), 46.21 (CH_2 of Et_3N), 119.72 ($C_{2,6}$), 125.70 (C_4), 138.40 ($C_{3,5}$-CH_3), 152.58 (C_1–O); ^{31}P NMR ($CDCl_3$, ppm): 106.78 (s)
5	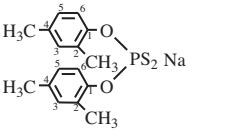	^{1}H NMR (DMSO-d_6, ppm): 2.07 (s, 6H, 2-CH_3), 2.17 (s, 6H, 4-CH_3), 6.47 (d, J = 8 Hz, 2H, H_5), 6.73 (s, 2H, H_3), 6.80 (d, J = 8 Hz, 2H, H_6); ^{13}C NMR (DMSO-d_6, ppm): 17.00 (2-CH_3), 19.72 (4-CH_3), 117.66 (C_6), 122.74 (C_2–CH_3), 126.70 (C_5), 127.25 (C_4–CH_3), 131.01 (C_3), 161.97 (C_1–O); ^{31}P NMR (DMSO-d_6, ppm): 107.48 (s)
6	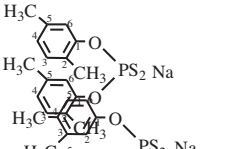	^{1}H NMR (DMSO-d_6, ppm): 2.23 (s, 6H, 2-CH_3), 2.28 (s, 6H, 5-CH_3), 6.82 (d, J = 7.6 Hz, 2H, H_3), 7.11 (d, J = 7.6 Hz, 2H, H_4), 7.47 (s, 2H, H_6); ^{13}C NMR (DMSO-d_6, ppm): 17.12 (2-CH_3), 20.32 (5-CH_3), 123.52 (C_6), 127.63 (C_4), 128.47 (C_2–CH_3), 131.62 (C_3), 137.42 (C_5–CH_3), 151.42 (C_1–O); ^{31}P NMR (DMSO-d_6, ppm): 106.62 (s)
7	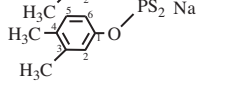	^{1}H NMR (DMSO-d_6, ppm): 2.15 (s, 6H, 4-CH_3), 2.16 (s, 6H, 3-CH_3), 6.97 (d, J = 7.6 Hz, 2H, H_6), 7.00 (s, 2H, H_2), 7.36 (d, J = 8 Hz, 2H, H_5); ^{13}C NMR (DMSO-d_6, ppm): 19.14 (4-CH_3), 20.01 (3-CH_3), 117.34 (C_6), 119.13 (C_2), 122.96 (C_4–CH_3), 127.84 (C_5), 136.62 (C_3–CH_3), 151.42 (C_1–O); ^{31}P NMR (DMSO-d_6, ppm): 107.31(s)
8	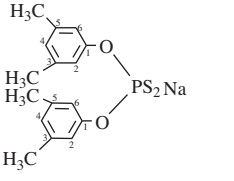	^{1}H NMR (DMSO-d_6, ppm): 1.99 (s, 12H, 3,5-$(CH_3)_2$), 6.54 (s, 4H, $H_{2,6}$), 6.73 (s, 2H, H_4); ^{13}C NMR (DMSO-d_6, ppm): 23.12 (3,5-$(CH_3)_2$), 122.56 ($C_{2,6}$), 128.64 (C_4), 142.33 ($C_{3,5}$-CH_3), 154.53 (C_1–O); ^{31}P NMR (DMSO-d_6, ppm): 106.59 (s)

(*Continued*)

Table 2. (*Continued*).

S. No.	Compounds	^{1}H, ^{13}C and ^{31}P Chemical shift (δ)
9	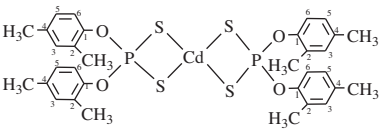	^{1}H NMR ($CDCl_3$, ppm): 2.20 (s, 12H, 2-CH_3), 2.36 (s, 12H, 4-CH_3), 7.01 (d, J = 8 Hz, 4H, H_6), 7.07 (d, J = 8 Hz, 4H, H_5), 7.37 (s, 4H, H_3); ^{13}C NMR ($CDCl_3$, ppm): 17.72 (2-CH_3), 20.81 (4-CH_3), 120.83 (C_6), 127.44 (C_2–CH_3), 129.96 (C_5), 132.13 (C_4–CH_3), 135.42 (C_3), 146.84 (C_1–O); ^{31}P NMR ($CDCl_3$, ppm): 101.46 (s)
10	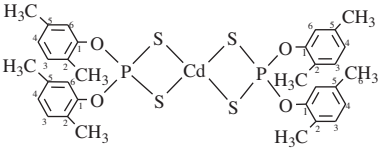	^{1}H NMR ($CDCl_3$, ppm): 2.27 (s, 12H, 2-CH_3), 2.29 (s, 12H, 5-CH_3), 6.96 (d, J = 7.6 Hz, 4H, H_3), 7.12 (d, J = 7.6 Hz, 4H, H_4), 7.31 (s, 4H, H_6) ppm; ^{13}C NMR ($CDCl_3$, ppm): 16.61 (2-CH_3), 20.99 (5-CH_3), 121.46 (C_6), 126.62 (C_4), 127.31 (C_2–CH_3), 131.24 (C_3), 136.91 (C_5–CH_3), 149.51 (C_1–O); ^{31}P NMR ($CDCl_3$, ppm): 101.26 (s)
11	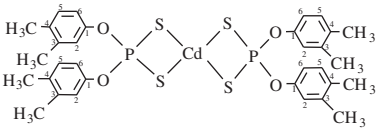	^{1}H NMR ($CDCl_3$, ppm): 2.28 (s, 12H, 4-CH_3), 2.31 (s, 12H, 3–CH_3), 6.86 (d, J = 7.6 Hz, 4H, H_6), 6.95 (s, 4H, H_2), 7.06 (d, J = 8 Hz, 4H, H_5); ^{13}C NMR ($CDCl_3$, ppm): 19.20 (4-CH_3), 19.93 (3-CH_3), 118.69 (C_6), 122.46 (C_2), 130.44 (C_4–CH_3), 133.88 (C_5), 138.10 (C_3–CH_3), 149.29 (C_1–O); ^{31}P NMR ($CDCl_3$, ppm): 101.02 (s)
12	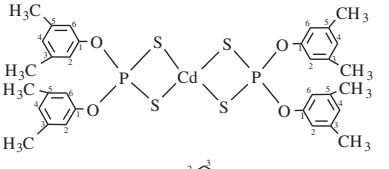	^{1}H NMR ($CDCl_3$, ppm): 2.35 (s, 24H, 3,5-$(CH_3)_2$), 6.77 (s, 8H, $H_{2,6}$), 7.00 (s, 4H, H_4); ^{13}C NMR ($CDCl_3$, ppm): 21.28 (3,5-$(CH_3)_2$), 119.35 ($C_{2,6}$), 126.58 (C_4), 138.95 ($C_{3,5}$-CH_3), 151.17 (C_1–O); ^{31}P NMR ($CDCl_3$, ppm): 101.86 (s)
13	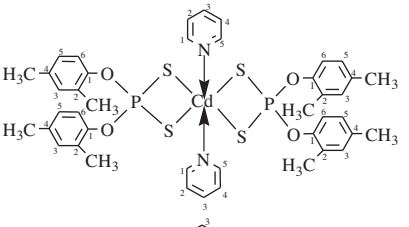	^{1}H NMR ($CDCl_3$, ppm): 2.18 (s, 12H, 2-CH_3), 2.25 (s, 12H, 4-CH_3), 7.00 (d, J = 8 Hz, 4H, H_6), 7.06 (d, J = 8 Hz, 4H, H_5), 7.26 (t, J = 14.4 Hz, 4H, $H_{2,4}$, C_5H_5 N), 7.35 (s, 4H, H_3), 7.68 (t, J = 13.6 Hz, 2H, H_3, C_5H_5 N), 8.52 (d, J = 8 Hz, 4H, $H_{1,5}$, C_5H_5 N); ^{13}C NMR ($CDCl_3$, ppm): 17.70 (2-CH_3), 20.78 (4-CH_3), 121.13 (C_6), 126.42 (C_2–CH_3), 128.31 (C_5), 131.26 (C_4–CH_3), 134.32 (C_3), 149.63 (C_1–O), 122.46, 136.41, 149.43 (C_5H_5 N); ^{31}P NMR ($CDCl_3$, ppm): 106.12 (s)
14	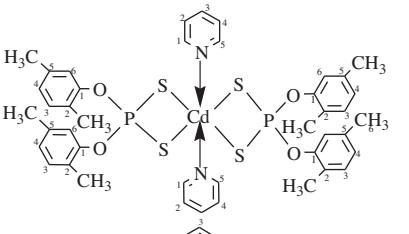	^{1}H NMR ($CDCl_3$, ppm): 2.19 (s, 12H, 2-CH_3), 2.24 (s, 12H, 5-CH_3), 6.94 (d, J = 7.6 Hz, 4H, H_3), 7.14 (d, J = 7.6 Hz, 4H, H_4), 7.24 (t, J = 14 Hz, 4H, $H_{2,4}$, C_5H_5 N), 7.29 (s, 4H, H_6), 7.62 (t, J = 12.8 Hz, 2H, H_3, C_5H_5 N), 8.51 (d, J = 8.4 Hz, 4H, $H_{1,5}$, C_5H_5 N); ^{13}C NMR ($CDCl_3$, ppm): 17.42 (2-CH_3), 19.63 (5-CH_3), 121.32 (C_6), 125.43 (C_4), 127.10 (C_2–CH_3), 130.46 (C_3), 135.42 (C_5–CH_3), 149.50 (C_1–O) 122.86, 136.23, 149.62 (C_5H_5 N); ^{31}P NMR ($CDCl_3$, ppm): 104.21(s)
15	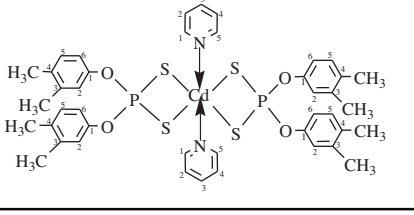	^{1}H NMR ($CDCl_3$, ppm): 2.14 (s, 12H, 4-CH_3), 2.17 (s, 12H, 3-CH_3), 6.98 (d, J = 7.6 Hz, 4H, H_6), 7.07 (s, 4H, H_2), 7.21 (t, J = 14.4 Hz, 4H, $H_{2,4}$, C_5H_5 N), 7.31 (d, J = 8 Hz, 4H, H_5), 7.66 (t, J = 14 Hz, 2H, H_3, C_5H_5 N), 8.55 (d, J = 8 Hz, 4H, $H_{1,5}$, C_5H_5 N); ^{13}C NMR ($CDCl_3$, ppm): 19.18 (4-CH_3), 19.89 (3-CH_3), 119.07 (C_6), 124.00 (C_2), 130.06 (C_4–CH_3), 132.87 (C_5), 137.46 (C_3–CH_3), 149.79 (C_1–O),122.90, 136.71, 149.69 (C_5H_5 N); ^{31}P NMR ($CDCl_3$, ppm): 106.11(s)

(*Continued*)

Table 2. (*Continued*).

S. No.	Compounds	^{1}H, ^{13}C and ^{31}P Chemical shift (δ)
16	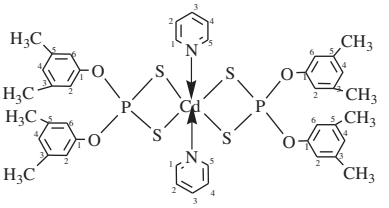	^{1}H NMR ($CDCl_3$, ppm): 2.31 (s, 24H, 3,5-$(CH_3)_2$), 6.86 (s, 8H, $H_{2,6}$), 7.03 (s, 4H, H_4), 7.28 (t, J = 14.4 Hz, 4H, $H_{2,4}$, C_5H_5 N), 7.77 (t, J = 13.6 Hz, 2H, H_3, C_5H_5 N), 8.50 (d, J = 4.4 Hz, 4H, $H_{1,5}$, C_5H_5 N); ^{13}C NMR ($CDCl_3$, ppm): 21.29 (3,5-$(CH_3)_2$), 119.48 ($C_{2,6}$), 126.88 (C_4), 139.08 ($C_{3,5}$-CH_3), 151.58 (C_1–O),124.38, 137.52, 149.60 (C_5H_5 N); ^{31}P NMR ($CDCl_3$, ppm): 104.23 (s)

Notes: s = singlet, d = doublet, q = quartet, m = multiplet.

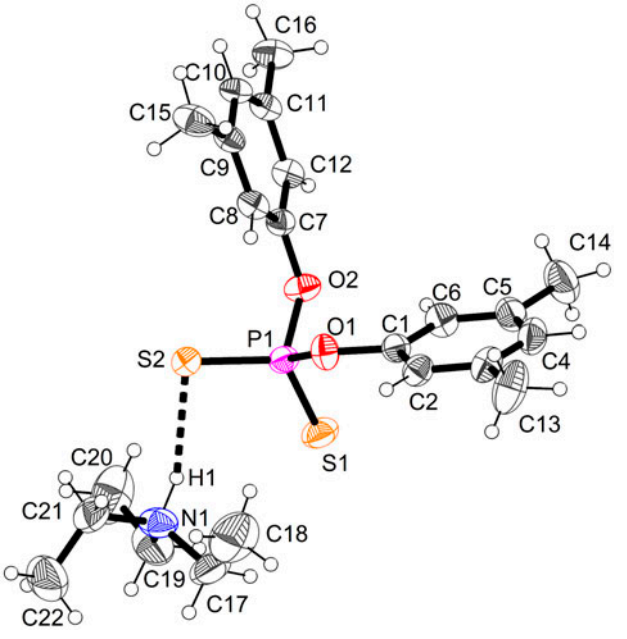

Figure 1. ORTEP view of **4** showing the atom-labeling scheme. Displacement ellipsoids are drawn at the 40% probability level.

with the values of 3.25(5) and 3.249(6) Å reported for $[Et_3NH]^+[(2\text{-}MeC_6H_4O)_2PS_2]^-$ [37] and $[Et_3NH]^+[(\overline{OCH_2CMe_2CH_2O)P(S)(S)}]^-$ [38], respectively.

P1–S1 and P1–S2 bond lengths in **4** [P1–S1 = 1.9389(12) and P1–S2 = 1.9586(12) Å] are comparable with the lengths of a single (2.14 Å) and double (1.94 Å) P–S bond [19]. In **16**, phosphorus–sulfur bonds [P1–S1 = 1.9759(8) and P1–S2 = 1.9779(8) Å] are intermediate between single and double P–S bonds, which suggests that the negative charge is delocalized over the S–P–S fragment. The S1–P1–S2 bond angle in $\{(3,5\text{-}CH_3)_2C_6H_3O\}_2PS_2HNEt_3$ [119.31(6)°] is slightly smaller than those of another literature reported triethylammonium salt, $[Et_3NH]^+[CH_2\{6\text{-}t\text{-}Bu\text{-}4\text{-}Me\text{-}C_6H_4O\}_2P(S)(S)]^-$ [38].

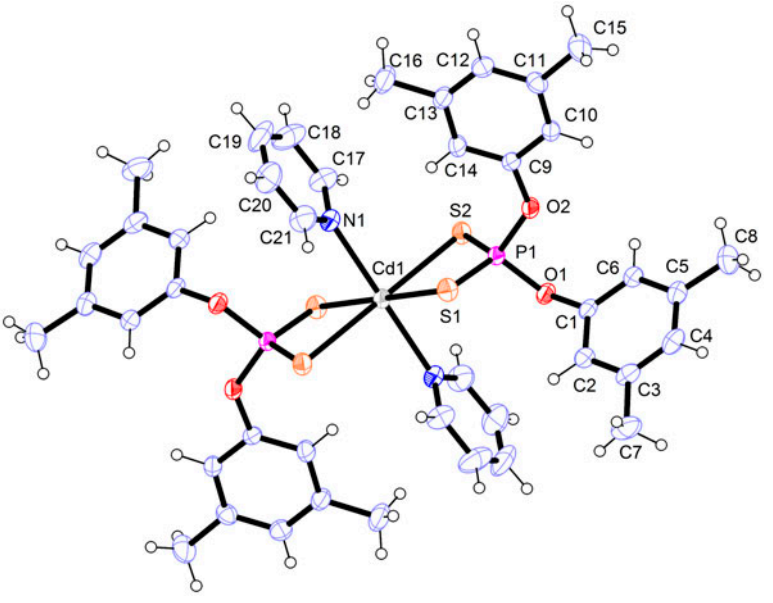

Figure 2. ORTEP view of **16** showing the atom-labeling scheme. Displacement ellipsoids are drawn at the 40% probability level.

Table 3. Selected bond lengths (Å) and angles (°) for **4**.

Bond distances			
P1–O1	1.610(2)	P1–O2	1.622(2)
P1–S1	1.9389(12)	P1–S2	1.9586(12)
O2–C7	1.386(4)	O1–C1	1.393(4)
N1–C19	1.471(5)	N1–C21	1.496(5)
N1–C17	1.538(6)	C20–C19	1.501(7)
Bond angles			
O1–P1–O2	102.33(12)	O1–P1–S1	112.57(10)
O2–P1–S1	105.96(9)	O1–P1–S2	104.41(9)
O2–P1–S2	111.06(9)	S1–P1–S2	119.31(6)
C7–O2–P1	127.09(19)	C1–O1–P1	129.01(19)
C19–N1–C21	116.1(4)	C19–N1–C17	110.5(4)
C21–N1–C17	112.7(3)	C2–C1–O1	115.3(3)
C6–C1–O1	123.7(3)	N1–C19–C20	112.8(4)
C18–C17–N1	113.0(4)	N1–C21–C22	114.1(3)

The crystal structure of **16** consists of two dithiophosphate and two pyridine units linked to cadmium. The coordination geometry is based on an octahedron within a *trans*-N_2S_4 donor set [figure 3(b)]. Cd(II) of **16** is surrounded by two chelating dithiophosphate anions, situated on a crystallographic center of inversion. The two pyridines are coordinated to cadmium axially. The cadmium attached to the pyridine ring is slightly above the plane of the pyridine ring (the value of the deviation being 0.2562). The dihedral angle between the pyridine ring (N1/C17/C18/C19/C20/C21) and the plane through cadmium (Cd1/S1/P1/S2)

Table 4. Important bond lengths (Å) and angles (°) for **16**.

Bond distances			
Cd1–N1	2.3973(19)		
Cd1–S1	2.7282(5)		
Cd1–S2	2.6741(5)		
P1–O1	1.5947(16)		
P1–O2	1.5943(16)		
P1–S1	1.9759(8)		
P1–S2	1.9779(8)		
O1–C1	1.407(3)		
O2–C9	1.398(3)		
N1–C21	1.324(3)		
N1–C17	1.321(3)		
Bond angles			
N1′–Cd1–N1	180.0	N1′–Cd1–S2	90.80(5)
N1′–Cd1–S2	89.20(5)	S2′–Cd1–S2	180.00(2)
N1′–Cd1–S1	87.48(5)	N1′–Cd1–S1′	92.52(5)
S2′–Cd1–S1′	76.336(17)	S2′–Cd1–S1	103.663(17)
N1′–Cd1–S1′	92.52(5)	S1′–Cd1–S1	180.000
S2′–Cd1–S1′	76.336(17)	O1–P1–S1	113.20(7)
O2–P1–O1	98.29(8)	O1–P1–S2	105.67(7)
S2–Cd1–S1	76.337(17)	S1–P1–S2	115.22(3)
O2–P1–S1	111.05(8)	P1–S1–Cd1	81.99(2)
O2–P1–S2	112.06(8)	C1–O1–P1	124.01(14)
C17–N1–C21	117.6(2)	C17–N1–Cd1	120.83(17)
P1–S2–Cd1	83.38(2)	C21–N1–Cd1	121.22(18)
C9–O2–P1	128.64(14)	N1–C17–C18	122.4(3)
N1–C21–C20	123.4(3)		

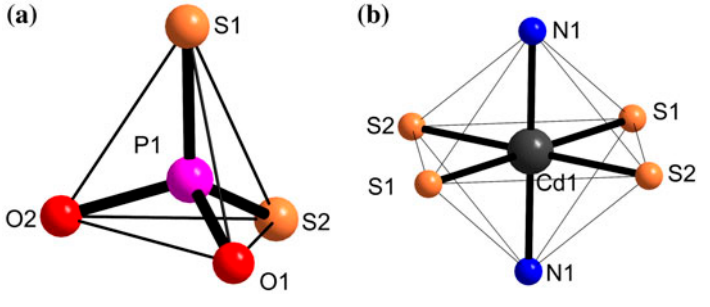

Figure 3. (a) Tetrahedral view of **4** and (b) Octahedral view of **16**.

is 78.72(1)°. The S1–Cd1–S2 and S1–P1–S2 angles [76.336(17)° and 115.22(3)°] are normal [39]. The Cd–S bonds lengths [2.7282(5) and 2.6741(5) Å] of **16** are in agreement with those reported for other analogous complexes $Cd\{S_2P(OCH_2CH_2Ph)_2\}_2 \cdot bipy$ [2.7958(14) and 2.5985(13) Å] [39], $Cd\{S_2P(OCy)_2\}_2$ [2.526(8) and 2.660(8)] [17], and $Cd[(^iPrO)_2PS_2]_2(py)_2$ [2.694(1) and 2.704(1)] [24]. The Cd–N bond distance in **16** is 2.397(19) Å which is comparable to the value found in $Cd[(^iPrO)_2PS_2]_2(py)_2$ [2.399(3) Å] [24]. The phosphorus is surrounded by two sulfurs and two oxygens to furnish a distorted tetrahedral geometry. The P–O bond in **16** is slightly shorter than those in **4**, although all of these are in the

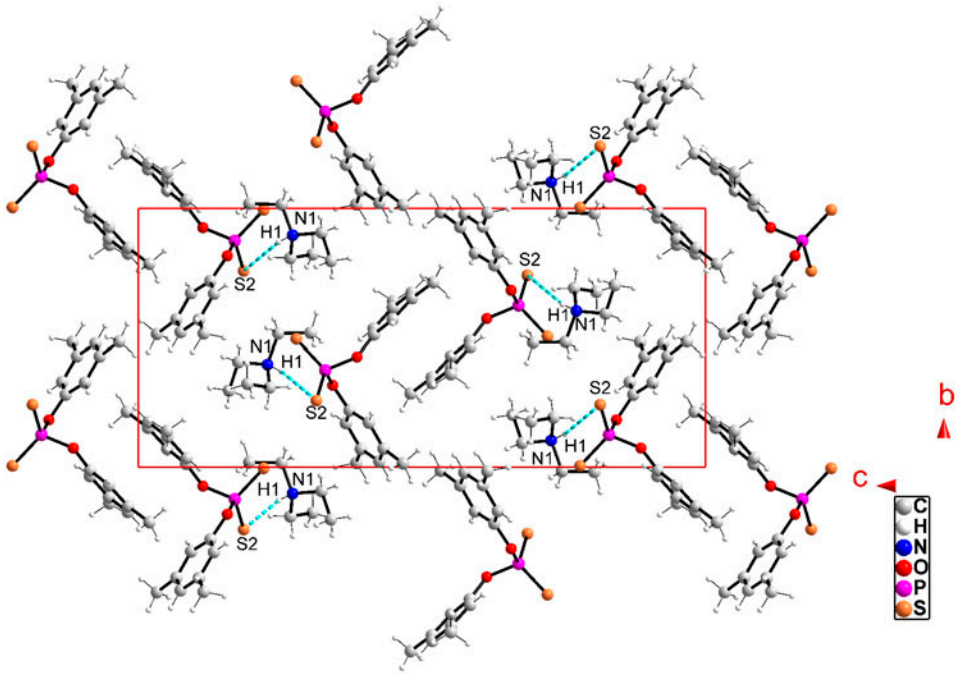

Figure 4. Packing diagram viewed down the *a*-axis for **4** showing hydrogen bonding.

Table 5. Geometry of intramolecular and intermolecular interactions for **4**.

D–H···A	D–H (Å)	H···A (Å)	D···A (Å)	θ [D–H···A (°)]
C6–H6···O2^{i}	0.930	2.50(2)	3.13(4)	124.8(2)
N1–H1···S2^{ii}	0.940	2.30(4)	3.20(3)	160.75(3)

Note: Symmetry codes: (i) x, y, z; (ii) $1-x$, $1/2+y$, $1/2-z$.

expected range. Compound **4** has only S2 involved in hydrogen bonding (table 5) while no classical hydrogen bonds are present in **16**.

3.4. *Thermogravimetric analysis*

The thermal behavior of $[\{(3,5\text{-}CH_3)_2C_6H_3O\}_2PS_2]_2Cd(NC_5H_5)_2]$ (**16**) displayed a thermolysis step that covers a temperature range from 150 to 900 °C (figure 5). The rate of weight loss increases steeply at 322 °C. The weight loss of 65.09% (Calcd wt. loss = 64.61%) corresponds to the formation of bis(dithio-*meta*-phosphato)cadmium(II) $[Cd(S_2PO)_2]$ which is diagnostic for dithiophosphate complexes [40]. The temperature range for formation of $[Cd(S_2PO)_2]$ is from 300 to 350 °C. The formation of final residue $CdSO_4$ contaminated with other thermolysis products was obtained with the weight loss of 77.60% (Calcd wt. loss = 77.95%) at 891 °C. The DTA curve shows an endotherm which signifies the thermal decomposition of the organic part of the dithiophosphate ligand at 160 °C.

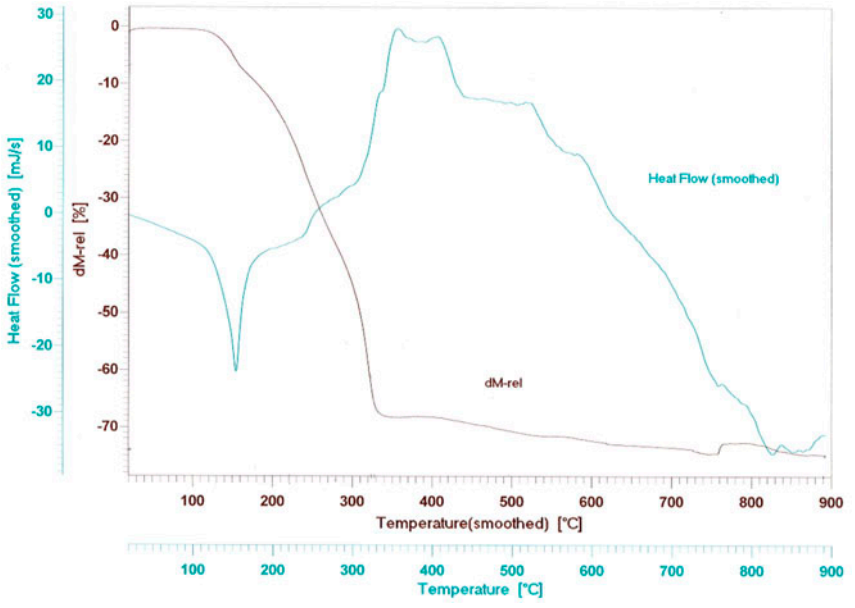

Figure 5. TGA/DTA curve of **16**.

4. Conclusion

We have synthesized and characterized new disubstituted diphenyldithiophosphates and their cadmium(II) complexes by elemental analysis, IR, NMR (^{1}H, ^{13}C and ^{31}P) and single-crystal X-ray analysis. In the triethylammonium salt $[\{(3,5\text{-}CH_3)_2C_6H_3O\}_2PS_2HNEt_3]$, phosphorus of the anion is tetrahedrally bonded to two S and two O atoms. The cation–anion N–H···S hydrogen bond interactions in **4** stabilized the structure. The complex $[\{(3,5\text{-}CH_3)_2C_6H_3O\}_2PS_2]_2Cd(NC_5H_5)_2$ has bidentate diphenyldithiophosphate ions with two sulfurs coordinated to cadmium. Each forms a four-membered chelate ring in the equatorial plane as a $[CdS_2]$ unit. Two pyridines are axially coordinated to cadmium.

Supplementary material

CCDC 971866 and 971951 contain the supplementary crystallographic data for **4** and **16**. These data can be obtained free of charge via http://www.ccdc.cam.ac.uk/conts/retrieving.html, or from the Cambridge Crystallographic Data Center, 12 Union Road, Cambridge CB2 1EZ, UK; Fax: (+44) 1223-336-033 or E-mail: deposit@ccdc.cam.ac.uk.

Acknowledgments

The authors are grateful to the NMR laboratory Department of Chemistry, University of Jammu, Jammu for providing NMR spectral facilities (PURSE program). One of the authors (Rajni Kant) acknowledges the DST for the single-crystal X-ray diffractometer as a National Facility under Project No. SR/S2/CMP-47/2003.

References

[1] P. O'Brien, J.R. Walsh, I.M. Watson, M. Motevalli, L. Henriksen. *J. Chem. Soc., Dalton Trans.*, 2491 (1996).
[2] J. Cheon, D.S. Talaga, J.I. Zink. *J. Am. Chem. Soc.*, **119**, 163 (1997).
[3] M. Bochmann. *Chem. Vap. Deposit.*, **2**, 85 (1996).
[4] P. Yan, Y. Xie, Y. Qian, X. Liu. *Chem. Commun.*, 1293 (1999).
[5] D.W. Tomlin, T.M. Cooper, D.E. Zelmon, Z. Gebeyehu, J.M. Hughes. *Acta Cryst.*, **C55**, 717 (1999).
[6] J.P. Groten, P.J. van Bladeren. *Trends Food Sci. Technol.*, **5**, 50 (1994).
[7] H. Savolainen. *Ren. Fail.*, **17**, 483 (1995).
[8] H. Hattori. *Soil Sci. Plant Nutr.*, **37**, 39 (1991).
[9] M. Hiroki. *Soil Sci. Plant Nutr.*, **38**, 141 (1992).
[10] J. XianJun, L. YongMing, Z. QiGuo, W. ShengChun, W. LongHua, Q. XianLiang, S. Jing. *Soils*, **32**, 75 (2000).
[11] N. Milosevic, M. Govedarica, M. Jarak, N. Petrovic, S. Jevtic, B. Lazic. *Acta Horticul.*, **462**, 133 (1997).
[12] M.G. Cherian. *Environ. Health Perspect.*, **54**, 243 (1984).
[13] G.R. Gale, L.M. Atkins, E.M. Walker, A.B. Smith, M.M. Jones. *Ann. Clin. Lab. Sci.*, **14**, 137 (1984).
[14] L.A. Shinobu, S.J. Jones, M.M. Jones. *Acta Pharmocol. Toxicol.*, **54**, 189 (1984).
[15] J.A. McCleverty, S. Gill, R.S.Z. Kowalski, N.A. Bailey, H. Adams, K.W. Lumbard, M.A. Murphy. *J. Chem. Soc., Dalton Trans.*, 493 (1982).
[16] A.V. Ivanov, O.V. Loseva, M.A. Ivanov, V.A. Konfederatov, A.V. Gerasimenko, O.N. Antzutkin, W. Forsling. *Russ. J. Inorg. Chem.*, **52**, 1595 (2007).
[17] J.S. Casas, A. Castineiras, M.S. Garcia-Tasende, A. Sanchez, J. Sordo, E.M. Vásquez-López. *Polyhedron*, **14**, 2055 (1995).
[18] A.V. Ivanov, O.N. Antzutkin, W. Forsling, N.A. Rodionova. *Russ. J. Coord. Chem.*, **29**, 301 (2003).
[19] S.L. Lawton, G.T. Kokotailo. *Inorg. Chem.*, **8**, 2410 (1969).
[20] A.V. Ivanov, O.N. Antzutkin, W. Forsling, D. Bostrom, Y. Yegao, N.A. Rodionova. *Dokl. Phys. Chem. (Proc. Russ. Acad. Sci.)*, **387**, 299 (2002).
[21] A.V. Ivanov, A.V. Gerasimenko, O.N. Antzutkin, W. Forsling. *Inorg. Chim. Acta*, **358**, 2585 (2005).
[22] Q.-L. Hao, X.-J. Yang, F.-F. Jian, L. Lu, X. Wang, I.A. Razak, S. Chantrapromma, H.-K. Fun. *Acta Cryst.*, **C57**, 42 (2001).
[23] M. Shimoi, A. Ouchi, M. Aikawa, S. Sato, Y. Saito. *Bull. Chem. Soc. Jpn.*, **55**, 2089 (1982).
[24] F. Jian, H. Xiao, Y. Li, K. Jiao. *J. Chem. Cryst.*, **33**, 705 (2003).
[25] A. Kumar, K.R. Sharma, S.K. Pandey. *Phosphorus Sulfur Silicon Relat. Elem.*, **182**, 1023 (2007).
[26] A.I. Vogel. *A Textbook of Quantitative Inorganic Analysis*, 4th Edn, Longman, London (1978).
[27] Oxford Diffraction. *CrysAlis PRO*, Oxford Diffraction, Yarnton (2010).
[28] G.M. Sheldrick. *Acta Cryst.*, **A64**, 112 (2008).
[29] A.L. Spek. *Acta Cryst.*, **D65**, 148 (2009).
[30] M. Nardelli. *J. Appl. Cryst.*, **28**, 659 (1995).
[31] C.M.V. Stalhandske, I. Persson, M. Sandstrom, E. Kamienska-Piotrowicz. *Inorg. Chem.*, **36**, 3174 (1997).
[32] T. Li, Z.-H. Li, S.-M. Hu, S.-W. Du. *J. Coord. Chem.*, **59**, 945 (2006).
[33] M. Sonmez. *Turk. J. Chem.*, **25**, 181 (2001).
[34] K. Nakamoto. *Infra-red Spectra of Inorganic and Coordination Compounds*, Wiley-Interscience, New York (1970).
[35] C. Glidewell. *Inorg. Chim. Acta*, **25**, 159 (1977).
[36] L.J. Farrugia. *J. Appl. Cryst.*, **45**, 849 (2012).
[37] J.E. Drake, C.L.B. MacDonald, A. Kumar, S.K. Pandey, R. Ratnani. *J. Chem. Cryst.*, **35**, 447 (2005).
[38] K.C. Kumara Swamy, S. Kumaraswamy, S. Raja, K.S. Kumar. *J. Chem. Cryst.*, **31**, 51 (2001).
[39] B. Xie, Y.-M. Wang, L.-K. Zou, J. Wang, Y.-L. Li, X. Lin. *Chin. J. Struct. Chem.*, **32**, 1457 (2013).
[40] T.A. Rodina, A.V. Ivanov, A.V. Gerasimenko, I.A. Lutsenko, M.A. Ivanov, J.V Hanna, O.N. Antzutkin, V.I. Sergienko, *Polyhedron*, **30**, 2210 (2011).